Metallic State in Cubic FeGe Beyond Its Quantum Phase Transition

P. Pedrazzini,[1] H. Wilhelm,[2,*] D. Jaccard,[1] T. Jarlborg,[1] M. Schmidt,[2] M. Hanfland,[3] L. Akselrud,[4] H. Q. Yuan,[2,†] U. Schwarz,[2] Yu. Grin,[2] and F. Steglich[2]

[1]*DPMC, University of Geneva, 24 Quai Ernest-Ansermet, 1211 Genève 4, Switzerland*
[2]*Max Planck Institute for Chemical Physics of Solids, 01187 Dresden, Germany*
[3]*European Synchrotron Radiation Facility, 38043 Grenoble, Cedex, France*
[4]*Ivan Franko Lviv National University, Kyryl and Mephodiy Street 6, 79005 Lviv, Ukraine*

(Received 19 June 2006; published 24 January 2007)

We report on results of electrical resistivity and structural investigations on the cubic modification of FeGe under high pressure. The long-wavelength helical order ($T_C = 280$ K) is suppressed at a critical pressure $p_c \approx 19$ GPa. An anomaly at $T_X(p)$ and strong deviations from a Fermi-liquid behavior in a wide pressure range above p_c suggest that the suppression of T_C disagrees with the standard notion of a quantum critical phase transition. The metallic ground state persisting at high pressure can be described by band-structure calculations if zero-point motion is included. The shortest FeGe interatomic distance display discontinuous changes in the pressure dependence close to the $T_C(p)$ phase line.

DOI: 10.1103/PhysRevLett.98.047204 PACS numbers: 75.30.Kz, 61.20.Ne, 62.50.+p, 71.15.Mb

The electronic and magnetic properties of binary compounds crystallizing in the $B20$ structure, such as the monosilicides of Mn, Cr, Fe, and Co are an active topic of research in condensed matter physics. Among them, FeSi and MnSi have attracted renewed interest. FeSi is a semiconductor with a narrow gap $E_g \approx 80$ meV and due to its peculiar magnetic and optical properties at low temperature, T, it is sometimes referred to as Kondo insulator or correlated insulator [1,2]. Band-structure calculations reproduce the gap as well as the recently observed transition to a metallic phase in $FeSi_{1-x}Ge_x$ at a critical concentration $x_c \approx 0.25$ [3–5]. Accordingly, it was evident that FeGe is a rare case where external pressure, p, might induce an isostructural transition from a metallic to an insulating state.

MnSi and FeGe are prominent examples where the Dzyaloshinskii-Moriya interaction causes a modulation of the ferromagnetic structure as a consequence of the lack of inversion symmetry in the $B20$ structure (space group $P2_13$) [6]. In MnSi, the helical order occurs below $T_C = 29$ K. The modulation has a wavelength of 175 Å and the ordered moments of about $m = 0.4\mu_B$ (with μ_B the Bohr magneton) per Mn atom are perpendicular to the spiral propagation vector $\mathbf{k} \parallel [111]$ [7]. It is well established that the second order phase transition is driven first order for a sufficiently weak magnetic interaction close to the critical pressure, $p_c = 1.46$ GPa [7–10]. In a wide p range above p_c, MnSi presents unusual physical properties, such as non-Fermi-liquid (NFL) behavior in the electrical resistivity, $\rho(T) \propto T^{3/2}$ [11,12], or partial ordering suggesting a magnetic state at high p [13]. In FeGe, on the other hand, helimagnetism sets in through a first order phase transition at $T_C = 280$ K with a saturated moment of $m = 1\mu_B$ per Fe atom [14]. The helical modulation has a period of about 700 Å and propagates along [100]. It alters its direction to $\mathbf{k} \parallel [111]$ at $T_2 \approx 211$–245 K without a change in the period [15]. Given the structural and magnetic similarities between MnSi and FeGe, it seems very likely that a volume compression in FeGe could eventually suppress the long-range magnetic order and reveal strong deviations from the standard notion of a Landau-Fermi liquid (LFL).

Single crystals of cubic FeGe were grown by vapor transport in a two-zone furnace, using iodine as chemical agent [16]. FeGe crystallized very slowly by an endothermal transport reaction from 850 to 810 K. The largest pieces were examined thoroughly by various x-ray techniques and electron-beam microanalysis. Four-probe $\rho(T)$ measurements were carried out on a $690 \times 105 \times 23$ μm^3 parallelepiped with the current ($4 \leq j \leq 80$ A/cm^2) applied perpendicular to a [111] direction. The sample was mounted together with a strip of Pb, which served as p gauge, in a Bridgman-type high-pressure cell using steatite as a p-transmitting medium [17]. Additional low-p data were obtained using a second pressure cell. The x-ray diffraction experiments were performed on well ground and annealed powder (at 670 K for two days) using a diamond-anvil cell with helium as p medium and the fluorescence peaks of $SrB_4O_7:Sm^{2+}$ as p gauge [18].

Figure 1 shows the T dependence of the nonphononic resistivity, $\rho(T) - \rho_{ph}(T)$, of cubic FeGe. The phonon contribution, $\rho_{ph}(T)$, is described with the Bloch-Grüneisen formula using both p-independent Debye temperature, $\Theta_D = 250$ K, and amplitude, $\rho_{ph}(300\ \mathrm{K}) = 87\ \mu\Omega$ cm. For $p < 12$ GPa the sharp kink is attributed to T_C. An additional broad anomaly is resolved at T_2 up to 8 GPa. It seems to be associated with the sluggish change in the modulation vector observed at $p = 0$ [15]. Above $p \approx 12$ GPa, only T_C is detected and it decreases by an order of magnitude upon approaching 18.4 GPa (inset to Fig. 1). Slightly above this p, however, the slope change in $\rho(T)$ occurs at higher T and therefore we label it T_X.

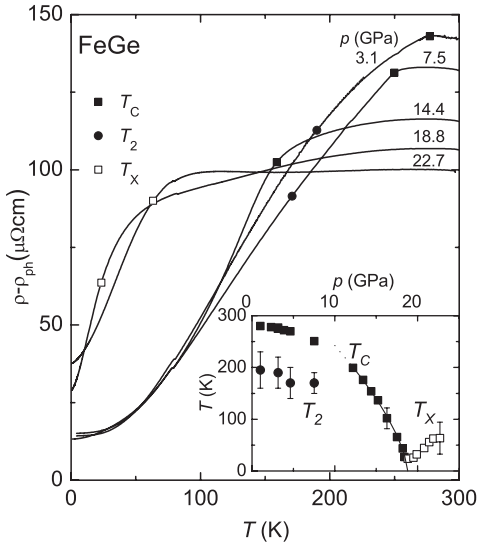

FIG. 1. Nonphononic contribution to the electrical resistivity in cubic FeGe, $\rho - \rho_{\mathrm{ph}}$. The onset of different spiral magnetic ordering at T_C and T_2 leads to anomalies in $\rho(T)$, indicated by the symbols. The nature of the anomaly at T_X is not known. Inset: (T, p) phase diagram of cubic FeGe.

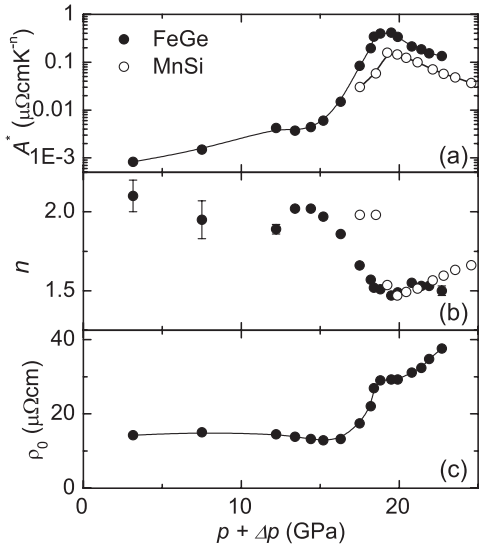

FIG. 2. Pressure-dependence of the resistivity parameters A^*, n, and ρ_0 in cubic FeGe. For comparison, MnSi data for A^* and n taken from Ref. [12] are included but shifted by $\Delta p = 17.3$ GPa to match p_c of FeGe.

Surprisingly, T_X increases steadily with p. We want to stress that at p as high as 19 GPa, unavoidable strain or p-gradients could obscure two adjacent anomalies in $\rho(T)$ and impede the precise detection of $T_C(p)$ below 25 K [19]. Although the residual resistivity has doubled upon reaching 23 GPa, FeGe remains metallic. For $p > 12$ GPa, $\rho(T)$ was measured down to 50 mK with low current densities and no hints of superconductivity were found. The (T, p) phase diagram is depicted in the inset to Fig. 1. Fitting $T_C(p) = T_C(0)(1 - p/p_c)^{\nu}$ to the data for 12.2 GPa $\leq p \leq$ 18.4 GPa yields $T_C(0) = 400(20)$ K, $p_c = 18.8(1)$ GPa, and the exponent $\nu = 0.66(4)$. The latter is almost identical to the exponent found in MnSi [8] although $\partial T_c/\partial p$ close to p_c is about a factor 2.5 larger. Similar to MnSi, we anticipate the transition in FeGe to be weakly first order. Thus, by analogy, long-range helimagnetism in FeGe seems to be suppressed at $p_c = 18.8$ GPa. The origin of T_X cannot be inferred from $\rho(T)$ experiments, though a magnetic nature seems very likely. This notion is encouraged by the observation that for $T > T_X$ as well as above T_C the nonphononic electrical resistivity is almost T independent, as expected for spin-disorder resistivity.

The T variation of $\rho(T)$ for $T < 10$ K is described by $\rho(T) = \rho_0 + A^*T^n$, with ρ_0 the residual resistivity and A^*T^n accounting for electron-magnon and/or electron-electron scattering. Figure 2 shows that $\rho_0 \approx 14\ \mu\Omega\,\mathrm{cm}$ and the exponent $n \approx 2$ remain almost unchanged below $p \approx 15$ GPa, while the slow increase of $A^*(p)$ could reflect the enhanced electron-magnon scattering. For $p >$ 15 GPa, however, all parameters change drastically, and $A^*(p)$ as well as $n(p)$ show striking similarities to MnSi close to its zero-T phase transition (open symbols in Fig. 2). Given the giant $A^*(p)$ maximum at p_c and the particular values for the exponents $\nu = 0.66$ and $n \approx 3/2$, it is tempting to associate p_c with a quantum critical point (QCP). The value $A^*(p_c) \approx 0.4\ \mu\Omega\,\mathrm{cm\,K}^{-1.5}$ is much larger than those measured in other $3d/4d$ itinerant ferromagnets close to a QCP, like Ni_3Al [20] or Ni_xPd_{1-x} [21]. It is even bigger than $A^*(p_c)$ in MnSi despite the larger p gradient expected at higher p. In a QCP scenario one would expect a narrow crossover regime where the LFL description breaks down. In FeGe, however, the exponent $n \approx 3/2$ remains p independent up to the highest p while $A^*(p)$ decreases rapidly. The strong increase of ρ_0 upon approaching p_c [Fig. 2(c)] can be interpreted as an enhanced impurity scattering due to ferromagnetic quantum fluctuations [22] whereas strong magnetic disorder or a near-lying insulating phase could be responsible for the steady increase of $\rho_0(p)$ above p_c. The similarity of our observations with those in MnSi [8,9,11] is striking and FeGe seems to be another candidate where features apparently related to a QCP manifest close to a weakly first order transition [11] into a metallic state with yet unknown magnetic properties [23].

The analysis of the low-T powder diffraction data provides some indications of a lattice instability close to a magnetic phase boundary. Figure 3 shows the shortest interatomic FeGe distance along the [111] direction, d_1, as obtained by a full profile refinement of the diffraction pattern. The low-p $d_1(p)$ behavior for 82 and 230 K described by an appropriate equation-of-state (EOS) clearly fails to account for the p dependence above 15 and 12 GPa, respectively. The two remaining FeGe distances as well as all distances at room temperature decrease smoothly with

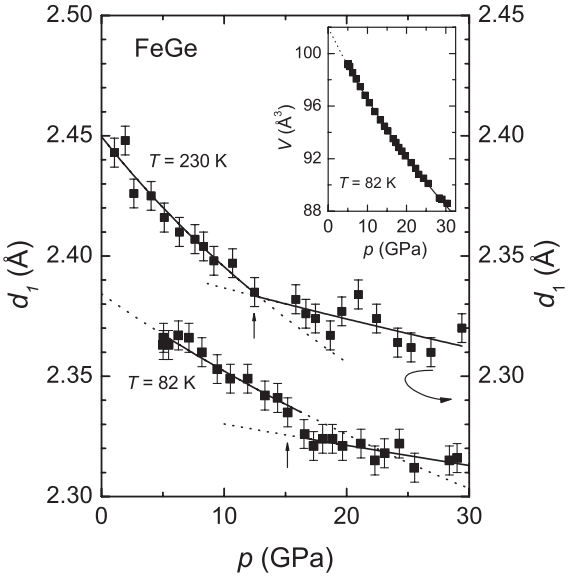

FIG. 3. Pressure dependence of the Fe-Ge distance d_1 at 82 K (left scale) and 230 K (right scale) in cubic FeGe. Lines are fits to the data and error bars represent 3 times the standard deviation. The vertical arrows indicate the onset of the anomaly in $d_1(p)$. Inset: $V(p)$ data and fit for $T = 82$ K.

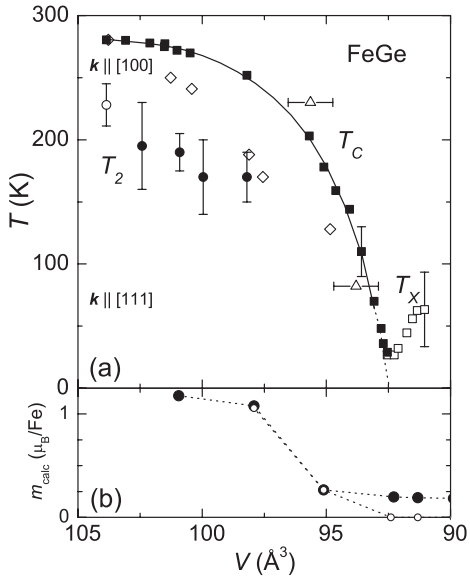

FIG. 4. (a) (T, V) phase diagram of cubic FeGe obtained from $\rho(T)$ and structural data (triangles). The T_2 data point (circle) at zero compression is taken from Ref. [15]. $T_C[V(x)]$ data on $FeSi_{1-x}Ge_x$ (diamonds) are taken from Ref. [3,27]. (b) Calculated magnetization m_{calc} with and without zero-point motion (bold and open symbols, respectively).

p. The anomalies in $d_1(p)$ agree remarkably well with the $T_C(p)$ phase boundary deduced from the $\rho(T)$ data (inset to Fig. 1) and pose the question about the nature of the phase transition observed in resistivity. Further investigations are necessary to clarify this point. The unit-cell volume, V, decreases continuously for all investigated T. As an example, data for $T = 82$ K are shown in the inset to Fig. 3. $V(p)$ can be described by a Murnaghan EOS [24], using a bulk modulus $B_0 = 147(3)$ GPa, its p derivative $B' = 4.4(2)$, and $V(0) = 102.43(7)$ Å^3 [25].

The structural information obtained at different T allows the (T, p) data (inset to Fig. 1) to be converted into the (T, V) phase diagram presented in Fig. 4(a). The change of compressibility with T was considered [25]. The anomalies in the FeGe distances are also added. They agree fairly well with the $T_C(V)$ phase boundary deduced from the $\rho(T)$ data. This accordance is remarkable if the quite different p environments are recalled (steatite vs helium). The smooth evolution of $T_C[V(p)]$ in FeGe resembles the one observed in MnSi. In both compounds $T_C(V) \rightarrow 0$ at a similar volume $V_c \approx 93$ Å^3, despite the subtle difference in the magnetic modulation, and NFL behavior is observed over a wide range of lattice compression. To our knowledge only one other metallic lattice, pure Fe, shows a similar behavior. In this case, a connection between correlated electron phenomena, including superconductivity, and the martensitic transition driven by magnetism has been considered [26].

The $T_C[V(x)]$ data of $FeSi_{1-x}Ge_x$ [3,27] are also included in Fig. 4. Although the initial suppression of T_C is stronger in $FeSi_{1-x}Ge_x$ than in FeGe, both systems have a similar T_C at $V \approx 95$ Å^3. At larger compression, however, a striking difference occurs: In $FeSi_{1-x}Ge_x$ long-range magnetic order disappears at a first order metal-to-insulator transition (MIT) [at $V(x_c) \approx 95$ Å^3 [27]] whereas $T_C(V)$ in FeGe still continuous to decrease. Furthermore, in FeGe, a metallic ground state is observed down to a compression comparable to the unit-cell volume of semiconducting FeSi at $p = 0$ ($V \approx 90$ Å^3).

We have addressed this unexpected result by performing self-consistent spin-polarized linear muffin-tin orbital (LMTO) calculations for lattice constants in the range 4.65 Å $< a <$ 4.08 Å, corresponding to a calculated p range 5 GPa $< p <$ 180 GPa. The first set of results in Ref. [5] were done without considering the effect of zero-point motion (ZPM). In the paramagnetic calculations the gap was found to increase steadily from $E_g \approx 15$ meV at the largest V to $E_g \approx 35$ meV at the smallest one, compared to $E_g \approx 80$ meV for FeSi [28]. The resulting magnetic moment per Fe atom, m_{calc}, follows rather closely the reduction of the measured $T_C(V)$ of FeGe [open symbols in Fig. 4(b)] and suggests a loss of magnetism around 92 Å^3, in contrast to our observations.

ZPM motion of atoms exists and it has been measured in FeSi [29], with a mean deviation of 0.03 Å, for $T \rightarrow 0$. The electronic band-structure calculations are preformed using static lattice distortions within the Born-Oppenheimer approximation. Unless there are high peaks or narrow gaps near E_F only minor effects of the ZPM occur on the electronic properties. In the case of FeGe, however, it

might be important to consider ZPM when E_F is close to the narrow gap in the density of states (DOS). We investigate this by doing band calculations for a 64-atom supercell with randomly generated deviations around the perfect lattice due to ZPM (Gaussian shape, rms of 0.03 Å) [28]. Only minor effects of ZPM occur when FeGe is clearly metallic and magnetic, i.e., $V \gtrsim 93$ Å^3 [see Fig. 4(b)]. But for $V \lesssim 92.5$ Å^3, when $E_g \approx 27$ meV in the perfect structure, the ZPM is able to close the gap and cause magnetism. The small averaged moments, $m_{\mathrm{calc}} \approx 0.18$–$0.08\mu_B$, persist until a compression to $V \approx 83$ Å^3 which corresponds to $p \approx 40$–50 GPa. The moments are not uniformly distributed on the Fe atoms but can vary by a factor of 4 among the different Fe sites.

The main difference between band-structure calculations for FeGe with and without ZPM is that the gap has disappeared in the former case. Therefore, the persistence of magnetism at large compression can be the result of ZPM, which tends to push the MIT to higher p. Nevertheless, the nature of such magnetism should be different from that in clearly metallic high-DOS systems: Since the structure is continuously changing on a time scale given by the atomic ZPM, it is expected that also the local moment on each Fe will change in time. Lattice disorder may be the origin of phase inhomogeneity. This also has the effect of making the gap narrower, but without the dynamic effects of ZPM. It is worth mentioning that for MnSi an inhomogeneous magnetic phase has been reported slightly above p_c [30], supporting the idea that ferromagnetic droplets can lead to an anomalous metallic behavior [11]. In FeGe for even larger compression, i.e., far above p_c, E_g will widen further and approach the situation in FeSi, where ZPM has no effect.

In conclusion, the electrical resistivity and structural data provide evidence for the suppression of the long-range magnetic order in cubic FeGe at $p_c \approx 19$ GPa though at higher p an anomaly at T_X might indicate some kind of magnetic correlations. The abrupt changes in the p dependence of the shortest FeGe distance may mark the beginning of a lattice instability which is in good agreement with the weakly first order $T_C(p)$ phase boundary. The metallic state, although with unusual properties, persists up to 23 GPa, the maximum p achieved in the $\rho(T)$ experiments. The wide p range of the non-Fermi-liquid behavior in connection with the exponent $n \approx 3/2$ and the giant value of the temperature coefficient, A^*, is interpreted as a breakdown of the standard scenario of a quantum critical phase transition. The band-structure calculations show that zero-point motion can overcome the narrow gap expected in FeGe at moderate compression. A semiconducting ground state, however, is predicted at much larger lattice densities.

We acknowledge U. Burkhardt, R. Cardoso, Yu. Prots, R. Ramlau, W. Schnelle, and H. Zhang for cutting and characterizing the crystals. We are grateful to R. Demchneya and A. Wosylus for their commitment during the x-ray experiments and to Z. Fisk for enlightening discussions.

*Present address: Diamond Light Source Ltd., Chilton, Didcot, Oxfordshire, OX11 0DE, United Kingdom.
†Present address: Department of Physics, University of Illinois, Urbana, IL 61801, USA.

[1] G. K. Wertheim *et al.*, Phys. Lett. **18**, 89 (1965).
[2] Z. Schlesinger *et al.*, Phys. Rev. Lett. **71**, 1748 (1993).
[3] S. Yeo *et al.*, Phys. Rev. Lett. **91**, 046401 (2003).
[4] V. I. Anisimov *et al.*, Phys. Rev. Lett. **89**, 257203 (2002).
[5] T. Jarlborg, J. Magn. Magn. Mater. **283**, 238 (2004).
[6] P. Bak and M. H. Jensen, J. Phys. C **13**, L881 (1980).
[7] B. Fåk *et al.*, J. Phys. Condens. Matter **17**, 1635 (2005).
[8] C. Thessieu *et al.*, Solid State Commun. **95**, 707 (1995); C. Thessieu, Ph.D. thesis, Université Paris VII, 1995.
[9] C. Pfleiderer, G. J. McMullan, S. R. Julian, and G. G. Lonzarich, Phys. Rev. B **55**, 8330 (1997).
[10] T. Vojta and R. Sknepnek, Phys. Rev. B **64**, 052404 (2001).
[11] N. Doiron-Leyraud *et al.*, Nature (London) **425**, 595 (2003).
[12] P. Pedrazzini *et al.*, Physica (Amsterdam) **B378–380**, 165 (2006).
[13] C. Pfleiderer *et al.*, Nature (London) **427**, 227 (2004).
[14] R. Wäppling and L. Häggström, Phys. Lett. A **28**, 173 (1968).
[15] B. Lebech, J. Bernhardt, and T. Freltoft, J. Phys. Condens. Matter **1**, 6105 (1989).
[16] M. Richardson, Acta Chem. Scand. **21**, 2305 (1967).
[17] D. Jaccard *et al.*, Rev. High Pressure Sci. Technol. **7**, 412 (1998).
[18] J. Leger, C. Chateau, and A. Lacam, J. Appl. Phys. **68**, 2351 (1990); F. Datchi, R. LeToullec, and P. Loubeyre, *ibid.* **81**, 3333 (1997).
[19] We estimate a p gradient $\Delta p \sim 0.5$ GPa from the 10%–90% criterion for the superconducting transition in Pb.
[20] P. G. Niklowitz *et al.*, Phys. Rev. B **72**, 024424 (2005).
[21] M. Nicklas *et al.*, Phys. Rev. Lett. **82**, 4268 (1999).
[22] K. Miyake and O. Narikiyo, J. Phys. Soc. Jpn. **71**, 867 (2002).
[23] U. K. Rößler, A. N. Bogdanov, and C. Pfleiderer, Nature (London) **442**, 797 (2006).
[24] F. D. Murnaghan, Proc. Natl. Acad. Sci. U.S.A. **30**, 244 (1944).
[25] The $V(p)$ dependence at 230 K [290 K] is described with $B_0 = 135(1)$ GPa [130(1) GPa], $B' = 4.7(1)$, and $V_0 = 103.17(3)$ Å^3 [103.86(2) Å^3].
[26] A. T. Holmes *et al.*, J. Phys. Condens. Matter **16**, S1121 (2004).
[27] Z. Fisk (private communication).
[28] T. Jarlborg, Phys. Rev. B **59**, 15 002 (1999).
[29] L. Vočadlo, K. S. Knight, G. D. Price, and I. G. Wood, Phys. Chem. Miner. **29**, 132 (2002).
[30] W. Yu *et al.*, Phys. Rev. Lett. **92**, 086403 (2004).